

## 5.1.9 UNEVEN BIT WEIGHTING

*As reported in Reference 5.1.9-1, with slight flow modifications for incorporation into this report*

**Reference 5.1.9-1 - "Cassini Imaging Science Subsystem Analog-to-Digital Uneven Bit Weighting Report for the Wide and Narrow Angle Cameras", D. I. Brown, February 1997**

### 5.1.9.1 Introduction

As part of the Cassini Imaging Science Subsystem (ISS) Instrument Calibration Requirements (699-CAS-4-2036-CAL), the flight Narrow Angle Camera (NAC) and Wide Angle Camera (WAC) were characterized for the distribution of the output Digital Number (DN) as a function of the input signal to the analog-to-digital converter (ADC) in order to determine (ADC) uneven bit weighting. Test methodology, test data graphical summaries, and data analysis approach are presented in this report. Digital data filenames are also listed for the use of interested parties.

### 5.1.9.2 Errors in the Analog-to-Digital Conversion Process

Observing the histogram of an arbitrary image with a broad range of DN shows a periodic series of spikes centered at  $(2^m) \cdot n$  (where  $m$  and  $n$  are integers) and occurring over a span of several DN. The largest of the spikes appear where  $m$ , the bit level, is large, or at the greater significant bits in the digitized output. The cause for this is attributed to the comparator in the analog to digital (A/D) converter. The A/D converter used in both ISS cameras is the Maxim MX7672 which uses the process of successive approximations to digitize the data. Ideally, the A/D reference voltage ( $V_{ref}$ ) is divided and refined by an adjustable network of resistors, and compared to the analog input voltage from the CCD pixel in a process that iterates until the voltages compare to within  $V_{ref}/4096$ , or 1.22 mV in the ISS case, for each DN. During this process, the specific DN values at  $2^m$ , (e.g. 2048) are digitized by comparing the reference voltage across a single resistor, whereas nearby DN's (e.g. 2047) are digitized with the adjustable resistor network appropriately set. Switching between the two DN's seamlessly requires balancing the group of resistors to the single resistor to an accuracy of 1 part in  $10^4$ , which is difficult to achieve in a practical device. Thus the imbalance in resistances produces the spikes.

### 5.1.9.3 The General Process of the Data Analysis

First, a 'super' histogram is constructed from summing the raw histograms of many individual exposures. This provides the combined number of raw data samples for each DN. Normalizing the raw superhistogram with another superhistogram comprised of 'ideal' values expected under these experimental circumstances produces the so-called 'effective bin width' for each DN, where the effective bin width varies about 1, the ideal normalized bin width. The effective bin widths are then sequentially added to produce a curve of adjusted DN vs. detected (or ideal) DN, where the adjusted DN values are taken at the center of their effective bin widths placed in sequence. Plotting  $(DN_{adjusted} - DN_{detected})$  vs.  $DN_{detected}$  produces the discretization error, a very sensitive indicator of system performance.

The A/D correction is the first modification that should be made to each image as it arrives from ISS. Since it is in floating point format, the ISS' integer format will have to be converted to floating point to accommodate the correction.

#### ***5.1.9.4 Practical Issues Specific to the ISS Data Analysis***

The crux of the process is to determine a credible way to generate the ideal histogram with which to normalize the data. The way in which this is usually done is to smooth the raw data so as to take out any local irregularities, spikes, etc., while saving the larger-scale, more-smoothly-varying components of the data, and assuming that this smoothed version is a good approximation to the ideal. This corresponds to using a low-pass filter on the raw data. To help develop confidence in the results, it was globally demonstrated that the sum of the effective bin widths over the characteristic length of the filter was identical to its length in ideal bin widths, to within some small error. (This is equivalent to saying that the discretization error was zero, to within a small amount, over the characteristic length of the filter, and that this held true over the span of the data.) This ensured that the error in the process over the length of the filter was close to zero everywhere, and in a practical data analysis helped to choose an appropriate filter. Also, a repeated application of the filter should produce effective bin widths that are close (0.5% or better) to those produced with one filtering. It is appreciated that repeated applications of a filter will effect the resultant 'ideal' curve, but any credible numerical result should be stable and converge iteratively, and thus be relatively insensitive to any 'appropriate' subsequent filtering of the data.

In the analysis of all of the ISS data, a selection of smoothing techniques were experimented with: boxcar-averaging filters, gaussian filters, piecewise continuous low-order polynomials, digital filters, and others. A slew of filtering parameters, including characteristic length, were changed to try to find a useful filter(s). As different methods were tried, results varied significantly from one filter to the next, which did not instill confidence in the outcome resulting from their use. However, as the double-filtering and discretization-error criteria, mentioned above, were applied systematically, one digital filter with very specific parameters emerged clearly as superior to the rest. This will be discussed below. It turned out that the results were very sensitive to the discretization-error over the filter length. A bracket on the maximum error in one DN bin that could be tolerated was between 0.001 to 0.005 of a bin width, on average. For example, in several cases involving a 21 DN bin boxcar-averaging filter, the characteristic-length error had periodic variations on the order of a boxcar length in scale and which were marginally in excess of 0.5%. This produced inordinately large variations in the effective bin width in the region of variation. When the chosen digital filter whose characteristic-length error of typically 0.1 to 0.2% was applied to the same data, the variations vanished. This provided an upper bound on the acceptable error over the filter length.

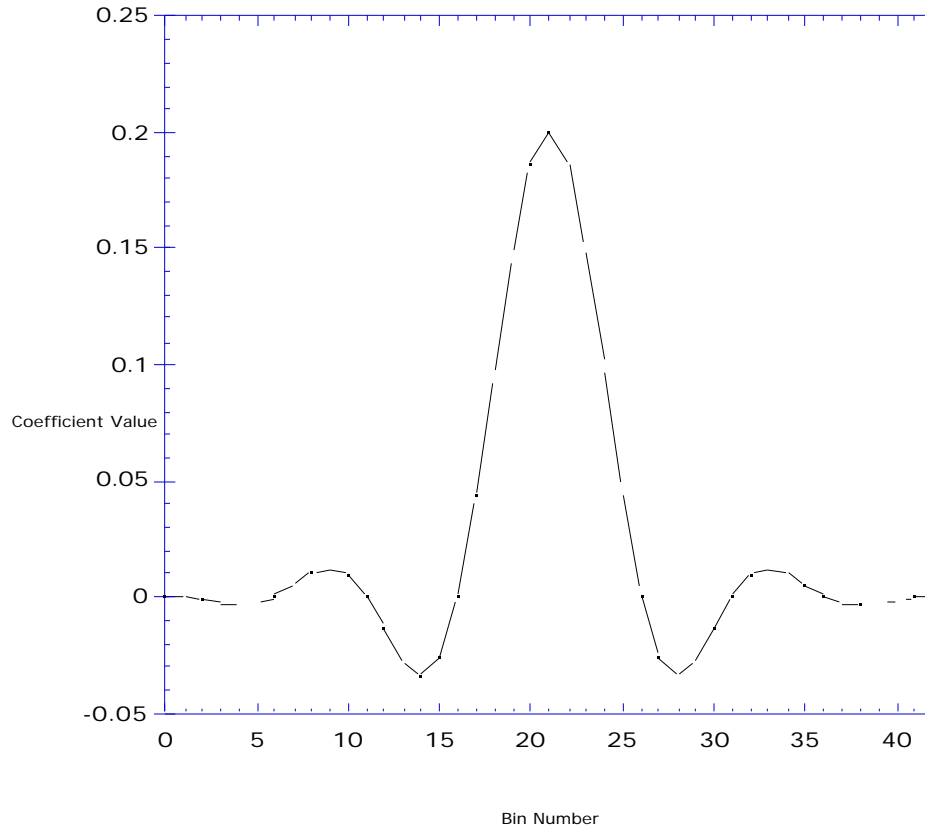
The software package used to analyze the ISS data was Interactive Data Language (IDL), version 4.0 for the Macintosh computer. Within IDL, the built-in digital filter function was used, specifically the 'digital\_filter(0.,0.2,50,21)' command, where the argument defines the filter characteristics, and will not be discussed here. However, the resultant digital filter profile is shown in Table 5.1.9.4-1, and is plotted in Figure 5.1.9.4-1. The filter should be normalized so that it does not modify the scale of the data it is applied to; that is, the sum of the values in the table should be 1.000000. In fact, they sum to about 0.998, and so must be modified slightly (multiplied by 1.00203) to accommodate for the error, which is significant for this analysis. Once modified, the filter is convolved with the raw data to produce the smoothed curve with the 'convol' command (with edge truncation turned on to handle the data at the very end of the chain, or in the 4070 DN region and up).

**Table 5.1.9.4-1- IDL Digital Filter Profile**

| <b>Bin Number</b> | <b>IDL Filter Value</b> |
|-------------------|-------------------------|
| 0.0000            | 0.00048715              |
| 1.0000            | 0.0000                  |
| 2.0000            | -0.0011762              |
| 3.0000            | -0.0026892              |
| 4.0000            | -0.0036594              |
| 5.0000            | -0.0029918              |
| 6.0000            | 0.0000                  |
| 7.0000            | 0.0049261               |
| 8.0000            | 0.010002                |
| 9.0000            | 0.012419                |
| 10.000            | 0.0094540               |
| 11.000            | 3.4456e-09              |
| 12.000            | -0.014156               |
| 13.000            | -0.028010               |
| 14.000            | -0.034412               |
| 15.000            | -0.026393               |
| 16.000            | -4.9601e-09             |
| 17.000            | 0.043465                |
| 18.000            | 0.096844                |
| 19.000            | 0.14863                 |
| 20.000            | 0.18625                 |
| 21.000            | 0.20000                 |
| 22.000            | 0.18625                 |
| 23.000            | 0.14863                 |
| 24.000            | 0.096844                |
| 25.000            | 0.043465                |
| 26.000            | -4.9601e-09             |
| 27.000            | -0.026393               |
| 28.000            | -0.034412               |
| 29.000            | -0.028010               |
| 30.000            | -0.014156               |
| 31.000            | 3.4456e-09              |
| 32.000            | 0.0094540               |
| 33.000            | 0.012419                |
| 34.000            | 0.010002                |
| 35.000            | 0.0049261               |
| 36.000            | 0.0000                  |
| 37.000            | -0.0029918              |
| 38.000            | -0.0036594              |
| 39.000            | -0.0026892              |
| 40.000            | -0.0011762              |
| 41.000            | 0.0000                  |
| 42.000            | 0.00048715              |

Note : Multiply above IDL filter value by 1.00203 to produce the filter used in this analysis.

**Figure 5.1.9.4-1 - IDL Digital Filter Plot**



### 5.1.9.5 Histogram Data Generation

#### 5.1.9.5.1 Test Set-Up

The data for a given histogram image was generated by the Dynamic Ramp Target, or 'DyRT', which was placed at the focus of a collimator and illuminated by an integrating sphere light source. By opening the DyRT's linear shutter at a constant rate during an exposure, a ramp in DN was produced with a constant number of samples taken for each DN. This simple, unique concept was realized by a movable linear shutter blade connected to a DC motor by a screw with a dovetail slide to maintain mechanical integrity and stability during operation. The design was packaged to fit into the collimator's target holder. The DyRT is shown in Figure 5.1.9.5-1.

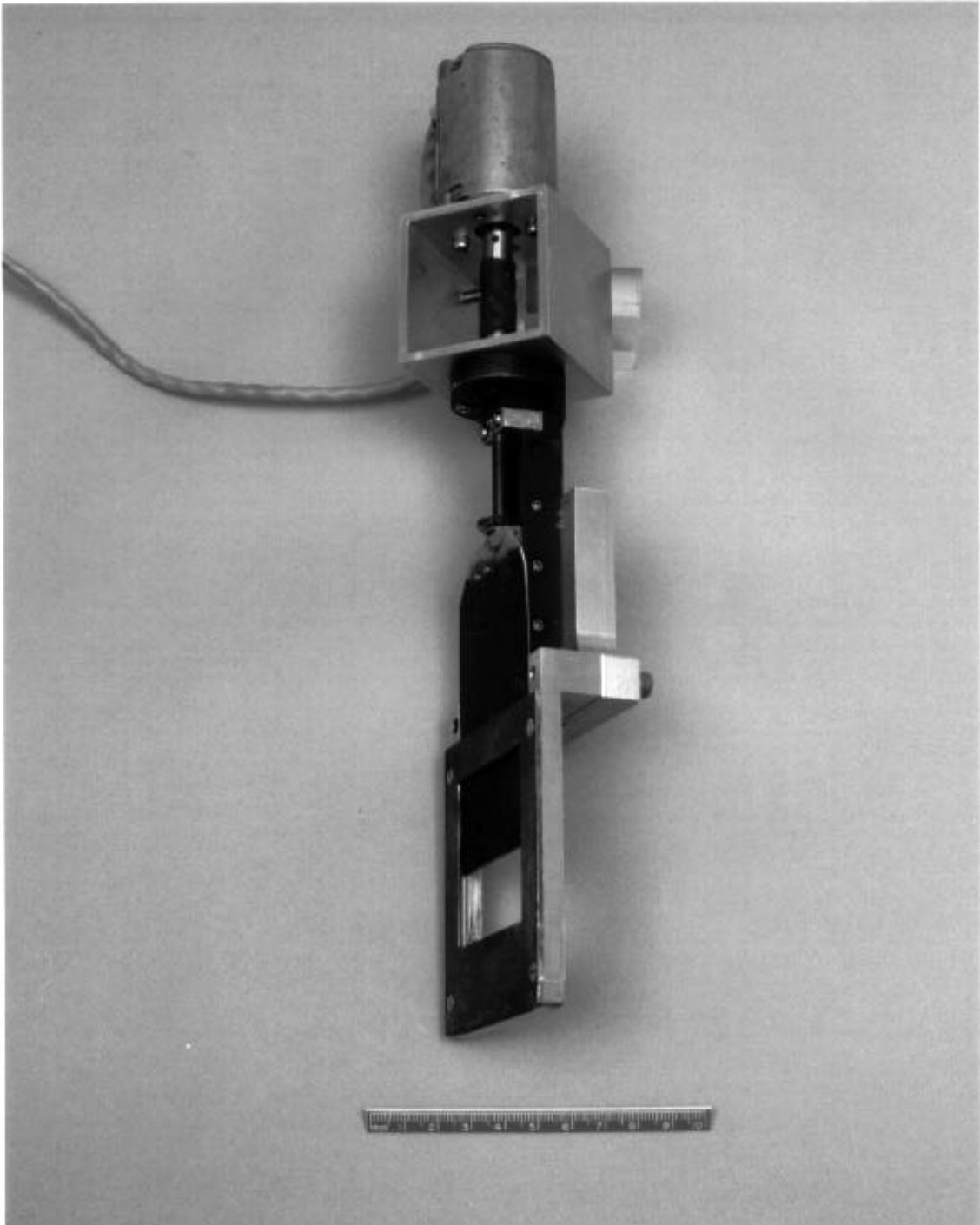


**Figure 5.1.9.5-1 - Dynamic Ramp Target (DyRT)**

### 5.1.9.5.2 Test Procedure

By varying the DC motor's voltage with a simple DC power supply, the speed of the motor could be changed, allowing the slope of the ramp to be adjusted. Similar adjustment of the light source's intensity varied the slope of the ramp as well. By harmonizing the two competing ramps, a plot of the total number of samples vs. DN across most of the 4096 DN range was gotten. Finally, the DyRT had to be timed to open during an ISS exposure. The obvious solution was to switch the DyRT on with a signal from the ISS shutter; this was not effected for various reasons. The next best solution was to open the ISS shutter for a long time (5.6 seconds), opening the DyRT during this interval. While this produced the data we see, it was not ideal for several reasons, primarily operational. The long ISS exposure time produced highly peaked data at the very low end (approximately 100 DN) of the DN scale due to low intensity light leaks in the system when the DyRT shutter was still closed. This made smoothing the data in this region problematic, requiring the effective bin widths to be set to one there.

### 5.1.9.5.3 Test Data

To produce a super histogram of about 10000 samples per DN, roughly one hundred images were required for each 1x1 binning (summing) case, and more for 2x2 binning. (The large number of samples were used to beat down any random A/D conversion error.) The 4x4 binning cases were not run due to fear of test equipment failure, lowest priority given to this case by the Science Team, and the inordinate amount of time required to perform the data gathering. For each case, the results of these exposures were processed and stored digitally as a table, with the first column of the table being DN value, from 0 to 4095, the second the number of samples vs. DN for the first image, etc. The specific calibration image numbers for the first to nth images are in the table header. Producing these tables automatically, once and for all, dramatically reduced the time necessary to analyze the data. While generating the raw data as expressed in the plots (with their corresponding digital data files), the data were scrutinized on an image-by-image basis to eliminate any undesirable peaks or files with missing lines in the data. Table 5.1.9.5-1 shows the super histogram file names assigned to each case.

**Table 5.1.9.5-1 - A/D Case vs. Histogram Table No.**

| DATA TYPE                           | FILENAME  |
|-------------------------------------|-----------|
| NAC/Gain State 1/2x2 Binning/-10 °C | ubw.tbl12 |
| NAC/Gain State 2/1x1 Binning/-10 °C | ubw.tbl6  |
| NAC/Gain State 2/1x1 Binning/+5 °C  | ubw.tbl8  |
| NAC/Gain State 3/1x1 Binning/-10 °C | ubw.tbl10 |
| WAC/Gain State 1/2x2 Binning/+5 °C  | ubw.tbl20 |
| WAC/Gain State 2/1x1 Binning-10 °C  | ubw.tbl15 |
| WAC/Gain State 2/1x1 Binning/+5 °C  | ubw.tbl18 |
| WAC/Gain State 2/1x1 Binning/+25 °C | ubw.tbl21 |
| WAC/Gain State 3/1x1 Binning/+5 °C  | ubw.tbl22 |

### ***5.1.9.6 Science Team Priority Assigned to Various Calibration Cases***

In the ISS Subsystem Level Calibration Requirement Document, 699-CAS-4-2036-CAL, no specific requirements were given regarding camera gain or binning state; calibration temperature was cited to be 'nominal', or +5 °C, while the A/D converter is sensitive to gain, binning, and camera temperature. (Note : The rate at which the analog data is converted to digital is the same, independent of the data transmission rate, and so the A/D iteration settling time is independent of the data rate for this system.) Discussion with R. West of the ISS Science Team established the following priority for both the NAC and WAC cameras:

Priority 1 : Gain state 2, 1x1 binning, nominal temperature (highest priority)

Priority 2 : Gain state 1, 2x2 binning, nominal temperature

Priority 3 : Gain state 3, 1x1 binning, nominal temperature

Priority 4 : Gain state 0, 4x4 binning, nominal temperature (if possible)

A decision based on practical issues prior to calibration ruled out the 4x4 binning case. The intent was to perform the calibration on cases 1) to 3) at -10, +5, and +25 °C.

Due to the way the overall NAC test sequence was laid out, the -10 degree A/D calibration data was generated first for all three cases . Subsequently, with severe time pressure on the overall ISS program, ISS management made a decision to cut the A/D testing short. The result is that for the NAC, cases 1) to 3) have been run for -10 °C, and case 1) has been run for +5 °C. It turned out that the A/D calibration data gathering takes an experienced team of two people several days to perform.

The WAC calibrations have cases 1) to 3) run at +5 °C, with case 1) run additionally at -10 and +25 °C.

### ***5.1.9.7 Output of the Calibration***

The graphical output of the analysis is included in this section of the report, with the raw data superhistogram, effective bin width, and discretization error shown for each of the above cases. Digital data for each of the above, as well as the adjusted DN's, are included as ASCII files using the naming convention specified below.

#### **5.1.9.7.1 Data Description**

##### ***5.1.9.7.1.1 Raw Superhistograms***

The ASCII file naming convention for the raw superhistogram data files is "camera\_raw\_gain.temp", (e.g. nac\_raw\_g2.p5). These files contain the summed raw histograms from the test data images (approximately 100 in all for 1x1 images, and 200 for the 2x2 images).

#### *5.1.9.7.1.2 Effective Bin Width Data*

The ASCII file naming convention for the effective bin width data files is “camera\_binw\_gain.temp”, (e.g. nac\_binw\_g2.p5). These files contain the effective bin width for the data from 0 to 4095 DN. There is a short region from 0 to approximately 200 DN where the effective bin widths are set to 1 artificially because raw data could not be smoothed in this region. The data generated have been filtered twice.

#### *5.1.9.7.1.3 Discretization Error*

The ASCII file naming convention for the discretization error data files is “camera\_error\_gain.temp”, (e.g. nac\_error\_g2.p5). These files contain the differences between the adjusted DN values and the detected (ideal) DN values.

#### *5.1.9.7.1.4 Adjusted DN Values*

The ASCII file naming convention for the adjusted DN values data files is “camera\_adjust\_gain.temp”, (e.g. nac\_adjust\_g2.p5).

## 5.1.9.7.2 Electronic Data Location

The names and locations of the electronic data files used for making this report are below in Table 5.1.9.7-1. All the electronic files are located on the Herschel machine and are downloadable per Appendix E.

| CAMERA | TEMP<br>°C | SUMMATION<br>MODE | GAIN<br>STATE | FILENAME          | DATA DESCRIPTION                   | FILE LOCATION<br>(@ <a href="http://herschel.jpl.nasa.gov">herschel.jpl.nasa.gov</a> ) |
|--------|------------|-------------------|---------------|-------------------|------------------------------------|----------------------------------------------------------------------------------------|
| NAC    | -10        | 2X2               | 1             | ubw.tbl12         | super histogram tables             | cassini:[calib_archive.nacfm.adc]                                                      |
| NAC    | -10        | 2X2               | 1             | nac_raw_g1.m10    | summed raw histograms              | scassini:[calib_archive.nacfm.adc]                                                     |
| NAC    | -10        | 2X2               | 1             | nac_binw_g1.m10   | effective bin width                | cassini:[calib_archive.nacfm.adc]                                                      |
| NAC    | -10        | 2X2               | 1             | nac_error_g1.m10  | discretization error               | cassini:[calib_archive.nacfm.adc]                                                      |
| NAC    | -10        | 2X2               | 1             | nac_adjust_g1.m10 | adjusted DN values                 | cassini:[calib_archive.nacfm.adc]                                                      |
| NAC    | -10        | 2X2               | 1             | "image no".img    | individual image data              | cassini:[nacfm.bit_weight]                                                             |
| NAC    | -10        | 1x1               | 2             | ubw.tbl6          | super histogram tables             | cassini:[calib_archive.nacfm.adc]                                                      |
| NAC    | -10        | 1x1               | 2             | nac_raw_g2.m10    | summed raw histograms              | scassini:[calib_archive.nacfm.adc]                                                     |
| NAC    | -10        | 1x1               | 2             | nac_binw_g2.m10   | effective bin width                | cassini:[calib_archive.nacfm.adc]                                                      |
| NAC    | -10        | 1x1               | 2             | nac_error_g2.m10  | discretization error               | cassini:[calib_archive.nacfm.adc]                                                      |
| NAC    | -10        | 1x1               | 2             | nac_adjust_g2.m10 | adjusted DN values                 | cassini:[calib_archive.nacfm.adc]                                                      |
| NAC    | -10        | 1x1               | 2             | "image no".img    | individual image data              | titan:[nacfm.bit_weight]                                                               |
| NAC    | 5          | 1x1               | 2             | ubw.tbl8          | super histogram tables             | cassini:[calib_archive.nacfm.adc]                                                      |
| NAC    | 5          | 1x1               | 2             | nac_raw_g2.p5     | summed raw histograms              | scassini:[calib_archive.nacfm.adc]                                                     |
| NAC    | 5          | 1x1               | 2             | nac_binw_g2.p5    | effective bin width                | cassini:[calib_archive.nacfm.adc]                                                      |
| NAC    | 5          | 1x1               | 2             | nac_error_g2.p5   | discretization error               | cassini:[calib_archive.nacfm.adc]                                                      |
| NAC    | 5          | 1x1               | 2             | nac_adjust_g2.p5  | adjusted DN values                 | cassini:[calib_archive.nacfm.adc]                                                      |
| NAC    | 5          | 1x1               | 2             | "image no".img    | individual image data              | titan:[nacfm.bit_weight]                                                               |
| NAC    | -10        | 1x1               | 3             | ubw.tbl10         | super histogram tables             | cassini:[calib_archive.nacfm.adc]                                                      |
| NAC    | -10        | 1x1               | 3             | nac_raw_g3.m10    | summed raw histograms              | scassini:[calib_archive.nacfm.adc]                                                     |
| NAC    | -10        | 1x1               | 3             | nac_binw_g3.m10   | effective bin width                | cassini:[calib_archive.nacfm.adc]                                                      |
| NAC    | -10        | 1x1               | 3             | nac_error_g3.m10  | discretization error               | cassini:[calib_archive.nacfm.adc]                                                      |
| NAC    | -10        | 1x1               | 3             | nac_adjust_g3.m10 | adjusted DN values                 | cassini:[calib_archive.nacfm.adc]                                                      |
| NAC    | -10        | 1x1               | 3             | "image no".img    | individual image data              | titan:[nacfm.bit_weight]                                                               |
| WAC    | 5          | 2X2               | 1             | ubw.tbl20         | super histogram tables             | cassini:[calib_archive.wacfm.adc]                                                      |
| WAC    | 5          | 2X2               | 1             | wac_raw_g1.p5     | summed raw histograms              | scassini:[calib_archive.wacfm.adc]                                                     |
| WAC    | 5          | 2X2               | 1             | wac_binw_g1.p5    | effective bin width                | cassini:[calib_archive.wacfm.adc]                                                      |
| WAC    | 5          | 2X2               | 1             | wac_error_g1.p5   | discretization error               | cassini:[calib_archive.wacfm.adc]                                                      |
| WAC    | 5          | 2X2               | 1             | wac_adjust_g1.p5  | adjusted DN values                 | cassini:[calib_archive.wacfm.adc]                                                      |
| WAC    | 5          | 2X2               | 1             | "image no".img    | individual image data              | titan:[wacfm.bit_weight]                                                               |
| WAC    | -10        | 1x1               | 2             | ubw.tbl15         | super histogram tables             | cassini:[calib_archive.wacfm.adc]                                                      |
| WAC    | -10        | 1x1               | 2             | wac_raw_g2.m10    | summed raw histograms              | scassini:[calib_archive.wacfm.adc]                                                     |
| WAC    | -10        | 1x1               | 2             | wac_binw_g2.m10   | effective bin width                | cassini:[calib_archive.wacfm.adc]                                                      |
| WAC    | -10        | 1x1               | 2             | wac_error_g2.m10  | discretization error               | cassini:[calib_archive.wacfm.adc]                                                      |
| WAC    | -10        | 1x1               | 2             | wac_adjust_g2.m10 | adjusted DN values                 | cassini:[calib_archive.wacfm.adc]                                                      |
| WAC    | -10        | 1x1               | 2             | "image no".img    | individual image data              | cassini:[wacfm.bit_weight]                                                             |
| WAC    | 5          | 1x1               | 2             | ubw.tbl18         | super histogram tables             | cassini:[calib_archive.wacfm.adc]                                                      |
| WAC    | 5          | 1x1               | 2             | wac_raw_g2.p5     | summed raw histograms              | scassini:[calib_archive.wacfm.adc]                                                     |
| WAC    | 5          | 1x1               | 2             | wac_binw_g2.p5    | effective bin width                | cassini:[calib_archive.wacfm.adc]                                                      |
| WAC    | 5          | 1x1               | 2             | wac_error_g2.p5   | discretization error               | cassini:[calib_archive.wacfm.adc]                                                      |
| WAC    | 5          | 1x1               | 2             | wac_adjust_g2.p5  | adjusted DN values                 | cassini:[calib_archive.wacfm.adc]                                                      |
| WAC    | 5          | 1x1               | 2             | "image no".img    | individual image data              | titan:[wacfm.bit_weight]                                                               |
| WAC    | 25         | 1x1               | 2             | ubw.tbl21         | super histogram tables             | cassini:[calib_archive.wacfm.adc]                                                      |
| WAC    | 25         | 1x1               | 2             | wac_raw_g2.p25    | summed raw histograms              | scassini:[calib_archive.wacfm.adc]                                                     |
| WAC    | 25         | 1x1               | 2             | wac_binw_g2.p25   | effective bin width                | cassini:[calib_archive.wacfm.adc]                                                      |
| WAC    | 25         | 1x1               | 2             | wac_error_g2.p25  | discretization error               | cassini:[calib_archive.wacfm.adc]                                                      |
| WAC    | 25         | 1x1               | 2             | wac_adjust_g2.p25 | adjusted DN values                 | cassini:[calib_archive.wacfm.adc]                                                      |
| WAC    | 25         | 1x1               | 2             | "image no".img    | individual image data              | titan:[wacfm.bit_weight]                                                               |
| WAC    | 5          | 1x1               | 3             | ubw.tbl22         | super histogram tables             | cassini:[calib_archive.wacfm.adc]                                                      |
| WAC    | 5          | 1x1               | 3             | wac_raw_g3.p5     | summed raw histograms              | scassini:[calib_archive.wacfm.adc]                                                     |
| WAC    | 5          | 1x1               | 3             | wac_binw_g3.p5    | effective bin width                | cassini:[calib_archive.wacfm.adc]                                                      |
| WAC    | 5          | 1x1               | 3             | wac_error_g3.p5   | discretization error               | cassini:[calib_archive.wacfm.adc]                                                      |
| WAC    | 5          | 1x1               | 3             | wac_adjust_g3.p5  | adjusted DN values                 | cassini:[calib_archive.wacfm.adc]                                                      |
| WAC    | 5          | 1x1               | 3             | "image no".img    | individual image data              | titan:[wacfm.bit_weight]                                                               |
| N/A    | N/A        | N/A               | N/A           | dig-filt.tab      | IDL digital filter<br>(unmodified) | cassini:[calib_archive.nacfm.adc]<br>cassini:[calib_archive.wacfm.adc]                 |

Table 5.1.9.7-1 - Electronic Data File Summary

### 5.1.9.7.3 Data Graphs

The graphs of the data described in 5.1.9.7.1 are linked below .

NAC / Gain 1 / 2x2 / -10 °C - Raw Histogram, Effective Bin Width, and Discretization Error

NAC / Gain 2 / 1x1 / -10 °C - Raw Histogram, Effective Bin Width, and Discretization Error

NAC / Gain 2 / 1x1 / +5 °C - Raw Histogram, Effective Bin Width, and Discretization Error

NAC / Gain 3 / 1x1 / -10 °C - Raw Histogram, Effective Bin Width, and Discretization Error

WAC / Gain 1 / 2x2 / +5 °C - Raw Histogram, Effective Bin Width, and Discretization Error

WAC / Gain 2 / 1x1 / -10 °C - Raw Histogram, Effective Bin Width, and Discretization Error

WAC / Gain 2 / 1x1 / +5 °C - Raw Histogram, Effective Bin Width, and Discretization Error

WAC / Gain 2 / 1x1 / +25 °C - Raw Histogram, Effective Bin Width, and Discretization Error

WAC / Gain 3 / 1x1 / +5 °C - Raw Histogram, Effective Bin Width, and Discretization Error

From the graphs, the following observations can be made :

- 1) The maximum discretization error value increases with temperature for the WAC flight camera.
- 2) The NAC is inconsistent with the WAC (per the limited data obtained) in that the maximum discretization error is lower at +5 °C than at -10 °C.
- 3) The average discretization error for both the WAC and the NAC over temperature is between 0.01-0.02 DN averaged over a continuous DN range of 1000 or more. The discretization plots are somewhat misleading for certain plots.
- 4) For the NAC, 2 out of 4 cases, from 3072 DN and up, there is an observable offset between 0.05 and 0.1 DN in the discretization error.
- 5) For the WAC, there is an observable offset from 0.1 to 0.2 DN in the discretization factor for 3 out of 5 cases above 3072 with one extending down to 2048. There was also unusual behavior in the standard deviation above 3072 DN of the discretization error in the remaining two cases.

### ***5.1.9.8 Concluding Remarks***

In general, there appears to be a minor offset in the data above 3072 DN in both the NAC and WAC . This is correctable using the adjusted A/D tables provided in this report in Section 5.1.9.7.1.4, Adjusted DN Values. The A/D correction is the first modification that should be made to each image as it arrives from ISS. This is done by substituting the adjusted DN values for the detected DN values. Since it is in floating point format, the ISS' integer format will have to be converted to floating point to accommodate the correction. Note that in the calibrated cases presented here, there was a large variability in the results for different temperatures (in a given camera). Therefore, the detected A/D values in the untested cases should not be modified in any way.